A Letters Journal Exploring the Frontiers of Physics

July 2007

EPL, **79** (2007) 26004 www.epljournal.org
doi: 10.1209/0295-5075/79/26004

Hydrodynamics and growth laws in lamellar ordering

M. Cencini[1,2], D. Diacono[3] and G. Gonnella[3,4]

[1] *INFM-CNR, SMC Dipartimento di Fisica Università Roma 1, P.zzle A. Moro 2, 00185 Roma, Italy*
[2] *ISC-CNR, Via dei Taurini 19, 00185 Roma, Italy*
[3] *Istituto Nazionale di Fisica Nucleare, Sezione di Bari - via Amendola 173, Bari, Italy*
[4] *Dipartimento di Fisica, Università di Bari - via Amendola 173, 70126 Bari, Italy*

received 5 April 2007; accepted in final form 4 June 2007
published online 2 July 2007

PACS 64.75.+g – Solubility, segregation, and mixing; phase separation
PACS 47.54.-r – Pattern selection; pattern formation
PACS 82.35.Jk – Copolymers, phase transitions, structure

Abstract – Ordering of lamellar phases described by a free-energy functional with short-range interactions is numerically investigated in two dimensions by means of a pseudo-spectral method. The ordering process is found to depend on the fluid viscosity: it is arrested for large viscosity values and proceeds as a power law for small ones, with a crossover regime for intermediate values. At varying the free energy parameters, strong evidence has been found that the ordering law, unlike binary mixtures, is not unique.

Introduction. – In many complex fluids the competition between attractive and repulsive interactions stabilizes pattern formation with modulated structures. Lamellar phases are a typical example observed, *e.g.*, in block copolymer melts [1], oil-water surfactant mixtures [2], supercooled liquids [3] and charged colloidal suspensions [4].

The formation of lamellar structures after a quench is characterized by the presence of defects and frustration on large scales [5]. The ordering process is thus typically slower than in ordinary binary mixtures and, sometimes, freezing is observed at late times. In simple binary mixtures different regimes with power law growth for the typical size of domains have been identified with exponents depending on the physical mechanism active during phase separation. In each regime universality of growth exponents is accepted (for a review see [6]). In lamellar systems the situation is far less clear and basic questions remain to be clarified. Recently, relations with the dynamics of structural glasses have been also pointed out [3,4,7].

In this letter we focus on the effects of hydrodynamics on lamellar ordering. In real systems indeed the velocity field, inducing motion around local or extended defects, is expected to play a relevant role on the ordering process. In particular, we consider a model based on a Ginzburg-Landau free-energy with short-range interactions, where dynamics is described by convection-diffusion and Navier-Stokes equations [8]. At equilibrium, this model is used to describe di-block copolymers in the weak segregation limit [9,10]. Simulations of this model for small size systems have shown that the presence of hydrodynamics is crucial to observe well-ordered lamellar domains. In ref. [8] the scale separation between the simulation box size and the lamellar period was of order 10. In more recent simulations with larger scale separation (~ 100) [11], for a limited set of free-energy parameters, slow logarithmic evolution was found at late times, and attributed to the formation of grain boundaries between differently oriented lamellae domains. Power law growth has been also found [12–19] for a variant of the model here considered with the lamellar phase induced by long-range interactions. This model, without hydrodynamics, has been also studied in relation with pattern formation in Raleight-Bénard cells above the convective threshold [20,21].

The aim here is to explore more widely the parameter space of the model studied in [8]. The main outcome of this study is that different ordering laws can be found for the same value of viscosity. This result indicates that in lamellar systems, differently from binary mixtures, growth properties depend on specific equilibrium characteristics of the system.

Model and basic equations. – The mixture under consideration is described by the free-energy [9]

$$F = \int \mathrm{d}\boldsymbol{r} \left[\frac{a}{2}\varphi^2 + \frac{b}{4}\varphi^4 + \frac{\kappa}{2}(\nabla\varphi)^2 + \frac{c}{2}(\nabla^2\varphi)^2 \right], \qquad (1)$$

φ being the order parameter that represents the concentration difference between the two components of the mixture. We take $b, c > 0$ to ensure stability. For $a > 0$ the fluid is disordered; for $a < 0$ and $\kappa > 0$ two homogeneous phases with $\varphi = \pm\sqrt{-a/b}$ coexist, as in usual binary mixtures [6]. A transition into a lamellar phase occurs for $\kappa < 0$. In the simplest approximation, assuming a profile $A \sin k_0 x$ for the direction transverse to the lamellae, one finds the transition ($|a| = b$) at $a \approx -1.11\kappa^2/c$ where $k_0 = \sqrt{-\kappa/2c}$ and $A^2 = 4(-a + \kappa^2/4cb)/3$ [11].

The system dynamics is ruled by the coupled set of equations

$$\partial_t u_\alpha + \boldsymbol{u}\cdot\boldsymbol{\nabla} u_\alpha = \nu\nabla^2 u_\alpha - \partial_\alpha p + \partial_\alpha\varphi(c\nabla^4\varphi - \kappa\nabla^2\varphi), \tag{2}$$

$$\partial_t\varphi + \boldsymbol{u}\cdot\boldsymbol{\nabla}\varphi = \Gamma\nabla^2\mu = \Gamma\nabla^2(a\varphi + b\varphi^3 - \kappa\nabla^2\varphi + c\nabla^4\varphi), \tag{3}$$

where we assumed an incompressible fluid velocity field $\boldsymbol{u}$ (*i.e.* $\boldsymbol{\nabla}\cdot\boldsymbol{u} = 0$) with a constant density equal to 1, and $\mu = \delta F/\delta\varphi$ is the chemical potential. Notice that the Laplacian in the r.h.s. of (3) ensures the conservation of φ. In the Navier-Stokes equation (2), ν is the kinematic viscosity; the pressure p includes all terms that can be expressed as gradient of a scalar function. The last two terms result from derivatives of the pressure tensor [8] or, equivalently, from the thermodynamic force $-\varphi\boldsymbol{\nabla}\mu$ (see, *e.g.*, refs. [22,23]). Equation (3) describes the advection of the order parameter and Γ is a mobility coefficient that sets the time scale of the interface diffusion.

We work on a two-dimensional square $L \times L$ domain with periodic boundary conditions. Equations (2) and (3) are integrated by using a standard pseudo-spectral algorithm with a 2/3-dealiasing scheme that was derived from a code used for simple binary mixtures [23] (see ref. [24] for more details on pseudo-spectral methods). Time integration is performed by a second-order Adam-Bashforth scheme with exact integration of the linear terms. The simulation grid consists of $N \times N$ collocation points (typically we used $N = 1024$ and 2048). Preliminary numerical tests were performed to establish the optimal space-step $\Delta x = L/N$ in order to have the largest system size with good resolution of the interface and of the small scale velocity features. For small viscosity we found that $\Delta x \approx 0.5$ satisfies such requirements. We checked, in systems of small size, that the equilibrium properties of the lamellar system (1) were correctly reproduced. One of the advantages of pseudospectral methods is that stability properties are rather robust, which is useful while varying the system parameters.

We performed a set of simulations varying ν and Γ. As for the parameters of the functional (1), we fixed $-a = b = 1$ while κ and c were varied while maintaining the system in the lamellar phase. Table 1 summarizes the simulation parameters used and labels the different runs that are discussed in the sequel.

Kinetics of lamellar ordering. – Let us first give a general picture of the ordering process of the lamellar system here considered. Runs start with zero velocity and a disordered configuration for the order parameter, obtained by randomly choosing $\varphi \in [-0.1 : 0.1]$ at each grid point. After the quench, for all values of the viscosity, lamellae evolve until the equilibrium wavelength is locally reached. At this stage the lamellae form a tangled pattern with many local defects. Later on, the system continues to order only at sufficiently low viscosity. An example of this behavior is shown in fig. 1, where we compare the time evolution of a low viscosity simulation (a) with a high viscosity one (b), holding fixed all the other parameters. As one can see, the patterns are very similar until $t \sim 100$ while, as time goes on, ordering proceeds with the formation of large domains of aligned lamellae only for low viscosity. On the contrary, for large viscosity, one observes almost frozen patterns of entangled lamellae with persistent defects. This confirms the importance of hydrodynamics for lamellar ordering as already described in previous simulations performed with lattice Boltzmann methods [8].

Table 1: Summary of simulations parameters: N^2 is the number of mesh points, $\Delta x = L/N$ the mesh step, ν the fluid viscosity, Γ the mobility, and c, κ free-energy parameters (we fixed $-a = b = 1$). The exponent α, explained in the text, is the growth exponent obtained by a best fit. The symbol A denotes arrested dynamics and N non-clear scaling (see text). When numbers are given the values are obtained by a least square fit on a time window variable from 1.5 to 2 decades, typically $t \in [500 : 60000]$ in the center of the scaling region. Run 5 and 5b were done starting from different initial conditions.

Run	N	Δx	ν	Γ	c	$-\kappa$	α
0	1024	1	10^1	1	2	2.47	A
1	1024	1	10^0	1	2	2.47	A
2	1024	0.5	10^{-1}	1	2	2.47	N
3	1024	0.5	0.075	1	2	2.47	N
4	1024	0.5	0.25	1	2	2.47	N
5	1024	0.5	10^{-2}	1	2	2.47	0.12(1)
5b	1024	0.5	10^{-2}	1	2	2.47	0.12(1)
6	1024	0.5	10^{-2}	0.1	2	2.47	0.12(3)
7	1024	0.5	10^{-2}	5	2	2.47	0.13(1)
8	1024	0.5	10^{-2}	10	2	2.47	0.11(2)
9	2048	0.5	10^{-2}	1	2	2.47	0.12(1)
10	2048	0.5	10^{-2}	1	2	1.43	0.20(2)
11	1024	0.5	10^{-2}	1	2	1.6	0.20(2)
12	1024	0.5	10^{-2}	5	2	1.6	0.19(2)
13	1024	0.5	10^{-2}	10	2	1.6	0.18(2)
14	2048	0.5	10^{-2}	1	2	1.6	0.20(2)
15	1024	0.5	10^{-2}	1	4	2.9	0.12(2)
16	2048	0.5	10^{-2}	1	4	2.9	0.13(3)
17	1024	0.5	10^{-2}	1	4	3.9	0.13(2)
18	1024	0.5	10^{-1}	1	4	4.9	N
19	1024	0.5	10^{-2}	1	4	4.9	0.19(2)
20	2048	0.5	10^{-2}	1	4	4.9	0.20(2)

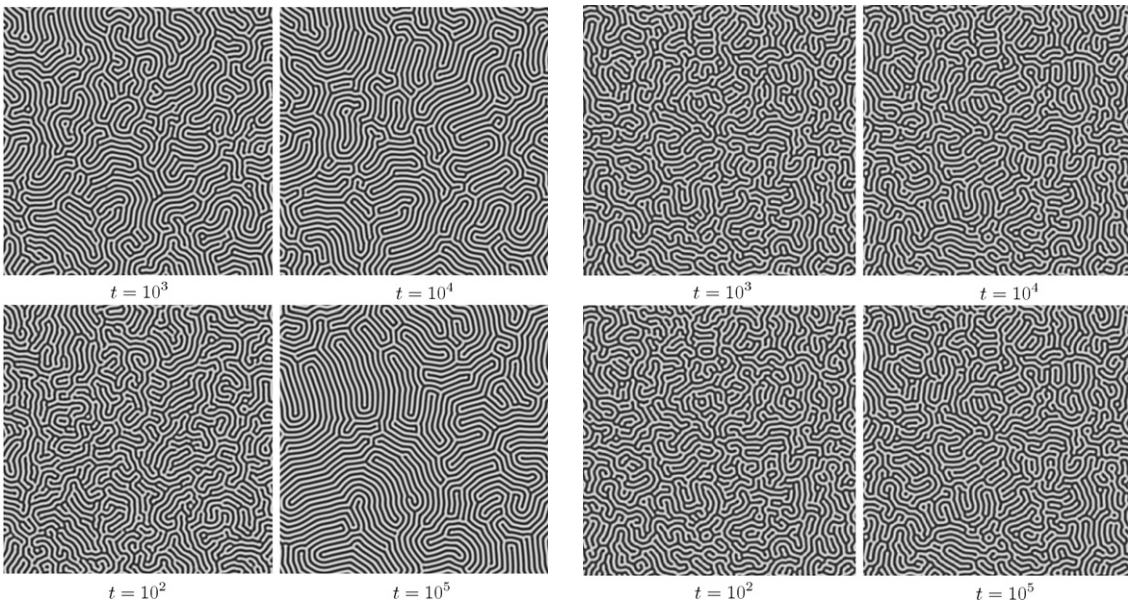

Fig. 1: (a) Snapshot of the order parameter for a portion 400×400 at four different times $t = 10^2, 10^3, 10^4, 10^5$ for run 9 that is $c = 2$, $\kappa = -2.47$ with $\nu = 0.01$. (b) The same for run 1, *i.e.* $c = 2$, $\kappa = -2.47$ with $\nu = 1.0$ (run 0 with $\nu = 10$ presents the same qualitative features).

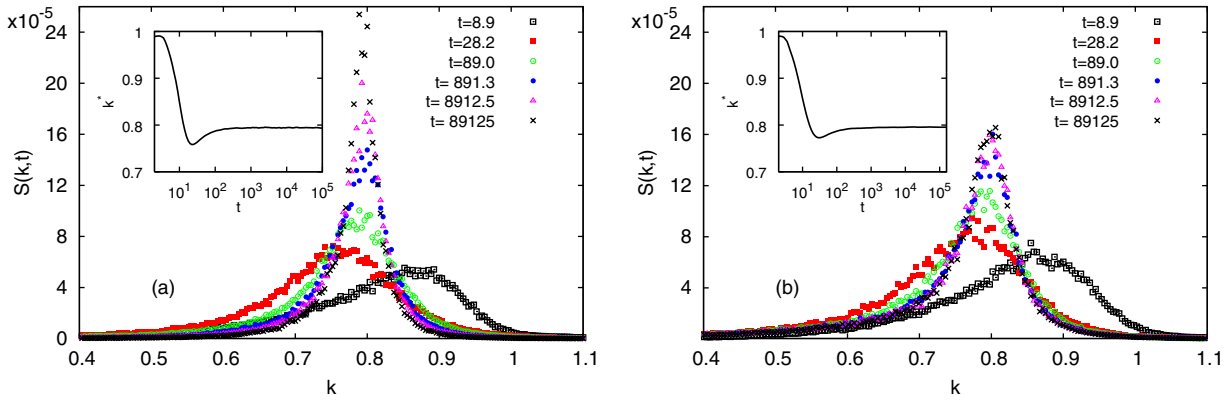

Fig. 2: (a) Order parameter structure factor $S(k,t)$ at different times (see legend) for run 9. Inset: time evolution of the peak position in the same run (this was evaluated as the peak position of the Lorentzian that best fits the structure factor). (b) The same for run 1.

A more quantitative insight into the ordering process can be obtained by looking at the evolution of the spherically averaged structure factor

$$S(k,t) = \langle \hat{\varphi}(\boldsymbol{k},t)\hat{\varphi}(-\boldsymbol{k},t)\rangle, \tag{4}$$

(where $\hat{\varphi}$ denotes the Fourier transform of the order parameter, and the brackets the average of a shell of radius $\boldsymbol{k}$), shown in fig. 2. In principle, in eq. (4), one should also perform an ensemble average over different initial conditions. However, for large system sizes as here, a self-average property can be assumed and checked in some cases (as in, *e.g.*, runs 5 and 5b). For both value of ν, in the early regime, $S(k,t)$ develops a maximum at a momentum k_M decreasing with time as in phase separation of usual binary mixtures. After k_M stabilizes on the equilibrium value k_0, further evolution is signalled by the increasing of the peak height together with a narrowing of its width, which is only observed in the low viscous case. As shown in the inset of fig. 2, the behavior of k_M is slightly more complex due to the presence of an undershoot before the stabilization to k_0. This undershoot seems to be originated by hydrodynamic effects, indeed it becomes less and less evident by increasing ν, and disappears when hydrodynamics is eliminated (not shown). A typical length scale of the system can be obtained from the inverse of the width of the structure factor, which can be estimated by approximating $S(k,t)$ as a squared Lorentzian [19]

$$S(k,t) = \frac{A^2(t)}{[(k^2 - k_M^2(t))^2 + B^2(t)]^2}\,, \tag{5}$$

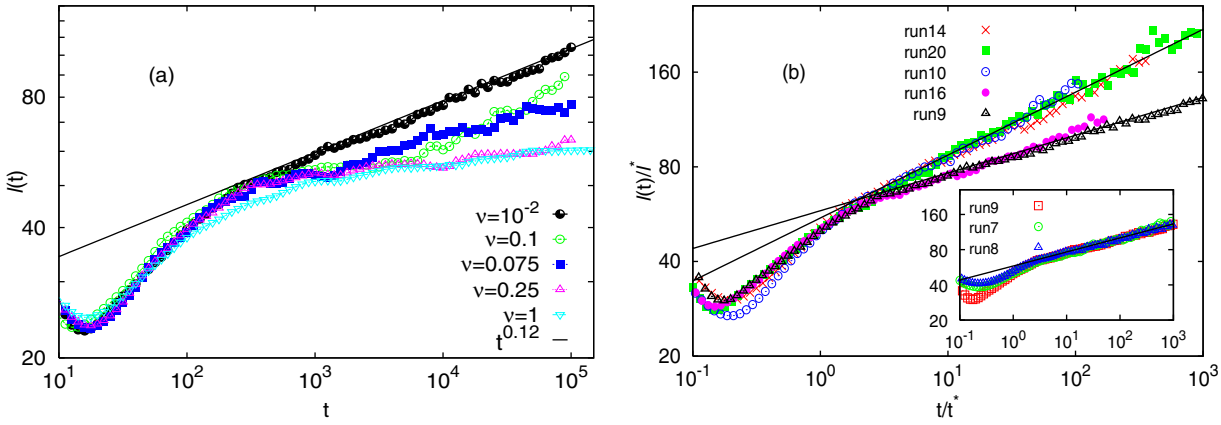

Fig. 3: (a) Inverse of the width of the structure factor, ℓ, *vs.* time for the runs $1, 2, 3, 4, 5$ (from bottom to top). The straight solid line displays the power law $\ell(t) \sim t^{0.12}$. Notice that for intermediate viscosities there is a crossover from arrested dynamics to growth with the crossover point that shift to longer times as ν get larger. (b) $\ell(t)/\ell^*$ *vs.* t/t^* for the runs $9, 10, 14, 16, 20$ (see table 1 for details). To compare the different runs we rescaled both ℓ and t with two factors ℓ^* and t^*, which have been chosen *ad hoc* to overlap the scaling ranges. At the first stage of the growth, a fair overlap of all curves is observed. At the late times two different laws emerges compatible with power laws with exponents 0.12 and 0.20 (shown in solid lines). Inset: the same as (b) for runs $7, 8, 9$ in which all parameters are fixed but Γ, see table 1; the straight line as slope 0.12.

where the width at half maximum is given by $\delta_k(t) = \sqrt{\sqrt{2}-1}B(t)/k_M^2(t)$ and the peak height by $S_p(t) = A^2(t)/B^4(t)$. The typical length scale is defined as $\ell(t) = 2\pi/\delta_k(t)$. At large times we found that both $S_p(t)$ and $\ell(t)$ behave in the same way with power law $S_p(t) \propto \ell(t) \propto t^\alpha$ in cases when lamellar ordering proceeds. The values of α in the different runs are summarized in table 1. As one can see we found two values $\alpha = 0.12$ and $\alpha = 0.2$. Data corresponding to $\alpha = 0.12$ could be also fitted with a logarithmic law. Previous simulations and theoretical arguments [7,11,14] suggest that logarithmic behaviour is related to the presence of extended defects (grain boundaries) between domains of lamellae differently oriented. However, our simulations do not show such kind of defects. Moreover, in all simulations interpreted with logarithmic behaviour as in [11], the configurations were practically not evolving at late times, which is not what we observe here. These considerations strengthen our interpretation in terms of a power law with $\alpha = 0.12$ (see fig. 3), which is further supported by the χ^2 probability which for the power law fit is bigger than in the case of the logarithmic fit.

The effects of viscosity on the ordering are summarized in fig. 3(a) where the time evolution of $\ell(t)$ is shown for different values of ν. Initially, the growth is similar for all values of ν. Later, for low viscosity ($\nu = 10^{-2}$), the growth continues with power law ($\ell(t) \sim t^{0.12}$ for the particular choice of free-energy parameters of runs 0-9) while, at the higher viscosity considered ($\nu = 1, 10$), the growth is practically arrested, and no further evolution can be appreciated, as seen in fig. 1(b). Intermediate cases ($\nu = 0.075, 0.1, 0.25$) show a crossover between the two behaviors: after an almost flat region $l(t)$ starts to grow at times which become longer as the viscosity becomes larger. It is possible that asymptotic growth always occurs, but that at very high viscosity it starts at times not reachable in simulations.

Growth laws. – Before presenting our results for the growth laws we recall that simulations for models with long-range interactions and without thermal fluctuations have suggested for the growth exponent the value $\alpha = 1/5$ [12–14,16,17,19] [1]. In the model under investigation, we considered values of κ and c such that the lamellar width $\lambda = 2\pi/k_0$ is between 7 and 12 to test whether the size of the lamellae can play a role in their ordering. We fixed two values of $c = 2, 4$ and varied κ and, to some extent, Γ as reported in table 1. Due to the computational costs, we could not explore more systematically the parameter space.

As reported in the table and already discussed, for all the explored values of the parameters we found at low viscosity, when the ordering proceeds, two different exponents $\alpha = 0.12$ and $\alpha = 0.20$. We did not find any clear trend able to explain the physical mechanism (if any) for the different exponents in relation with the lamellar thickness or other parameters. In fig. 3(b) we summarize the results for the largest runs. In particular we show the time evolution of $\ell(t)$ (the peak height S_p, not shown, provides the same information and, in the scaling range, can be superimposed to $\ell(t)$ by an appropriate multiplicative factor). The data obtained with different parameters have been superimposed by rescaling both the time and

[1] In these models, due to long-range interactions, ordering can also proceed without hydrodynamics; for a review see, *e.g.*, [17].

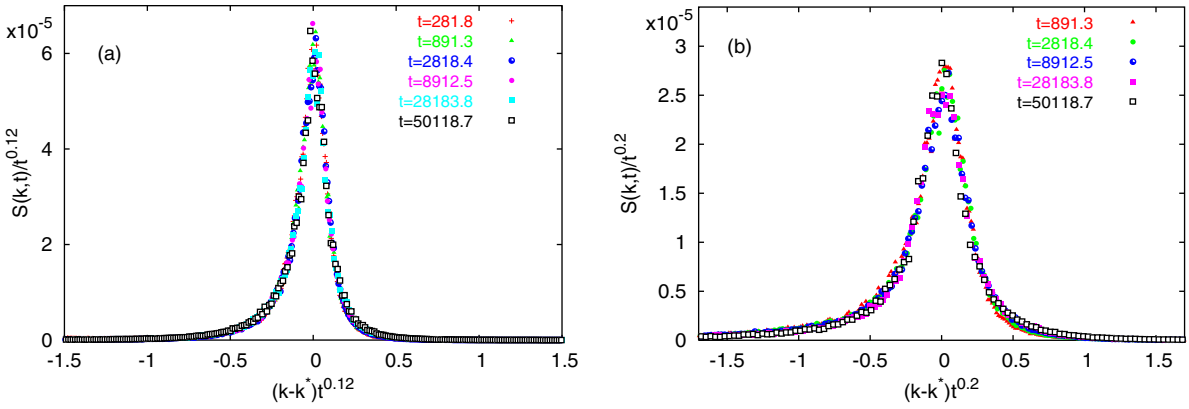

Fig. 4: Data collapse of the structure factor with the form $S(k,t) = t^{\alpha} f[(k-k^*)/t^{\alpha}]$ for (a) run 9 and (b) run 14. Different symbols (colors online) refer to different times. The exponents used for the collapse are $\alpha = 0.12$ and 0.2 in the case (a) and (b), respectively.

$\ell(t)$ by multiplicative factors t^* and ℓ^*, respectively[2]. We observed a fair overlap of all curves in the first stage of the dynamics, while in the scaling regime two different laws emerge as indicated by the two straight lines with exponents 0.12 and 0.20. As shown in the inset of fig. 3(b), the exponent does not seem to be sensitive to changes in the mobility Γ.

Finally, as shown in fig. 4, we verify that the structure factor satisfies the dynamical scaling relation [12]

$$S(k,t) = \ell(t) f[(k-k_0)\ell(t)]\,, \tag{6}$$

$f(x)$ being a scaling function. Notice that, to make the test even more severe, we did not use the measured $\ell(t)$ for collapsing the data but directly the power law behavior $\ell(t) \sim t^{\alpha}$ with the proper exponent $\alpha = 0.12$ or 0.20 for run 9 and 14, respectively. As one can see the collapse is rather convincing in both cases demonstrating the presence of dynamical scaling triggered by different exponents.

Final remarks. – The above results show that, at least in the framework of the free-energy here considered, the lamellar ordering dynamics cannot be characterized in terms of a unique exponent. Indeed, the evidence of two different exponents is fairly clear. We conclude by stressing the importance of hydrodynamics in the establishment of the scaling regime, and that the viscosity seems to set the length of a crossover from arrested evolution and the scaling regime.

* * *

MC acknowledges partial support from the PRIN "Statistical mechanics of complex systems" by MIUR, and CINECA for computational resources under the project "Turbulence in complex flows". GG acknowledges partial support from the PRIN "Rilassamenti lenti ed universalità: dalla materia soffice ai materiali granulari" by MIUR, and CINECA for computational resources under the project "Lattice Boltzmann Methods for liquid-vapour systems".

[2] Unfortunately the intrinsic difficulty of understanding the early regime of growth did not allow us to choose these rescaling parameters from first principles. Therefore we did an *ad hoc* choice by requiring the superposition of the knee between the early growth and the long time one t^{α}.

REFERENCES

[1] Bates F. S. and Fredrickson G., *Annu. Rev. Phys. Chem.*, **41** (1990) 525; Hamley I. W., *J. Phys.: Condens. Matter*, **13** (2001) R643.
[2] Gompper G. and Schick M., *Phase Transitions and Critical Phenomena*, Vol. **16** (Academic, New York) 1994.
[3] Grousson M., Krakoviack V., Tarjus G. and Viot P., *Phys. Rev. E*, **66** (2002) 026126.
[4] Tarzia M. and Coniglio A., *Phys. Rev. Lett.*, **68** (2006) 075702.
[5] Iwashita Y. and Tanaka H., *Phys. Rev. Lett.*, **95** (2005) 047801.
[6] Bray A. J., *Adv. Phys.*, **43** (1994) 357.
[7] Boyer D. and Viñals J., *Phys. Rev. E*, **65** (2002) 046119.
[8] Gonnella G., Orlandini R. and Yeomans J., *Phys. Rev. Lett.*, **78** (1997) 1695; *Phys. Rev. E*, **58** (1998) 480.
[9] Brazovskii S. A., *Sov. Phys. JETP*, **41** (1975) 85.
[10] Leibler L., *Macromolecules*, **13** (1980) 1602; Ohta T. and Kawasaki K., *Macromolecules*, **19** (1986) 2621; Fredrickson G. H. and Helfand E., *J. Chem. Phys.*, **87** (1987) 697.
[11] Xu A., Gonnella G., Lamura A., Amati G. and Massaioli F., *Europhys. Lett.*, **71** (2005) 651.
[12] Elder K. R., Viñals J. and Grant M., *Phys. Rev. Lett.*, **68** (1992) 3024.
[13] Cross M. C. and Meiron D. I., *Phys. Rev. Lett.*, **75** (1995) 2152.
[14] Hou Q., Sasa S. and Goldenfeld N., *Physica A*, **239** (1997) 219.
[15] Boyer D. and Viñals J., *Phys. Rev. E*, **64** (2001) 050101(R).

[16] Christensen J. J. and Bray A. J., *Phys. Rev. E*, **58** (1998) 5364.
[17] Qian H. and Mazenko G. F., *Phys. Rev. E*, **67** (2003) 036102.
[18] Harrison C. *et al.*, *Science*, **290** (2000) 1558; *Phys. Rev. E*, **66** (2002) 011706.
[19] Yokojima Y. and Shiwa Y., *Phys. Rev. E*, **65** (2002) 056308.
[20] Swift J. and Hohenberg P. C., *Phys. Rev. A*, **15** (1977) 319.
[21] Cross M. C. and Hohenberg P. C., *Rev. Mod. Phys.*, **65** (1993) 851.
[22] Ruiz R. and Nelson D. R., *Phys. Rev. A*, **23** (1981) 3224.
[23] Berti S., Boffetta G., Cencini M. and Vulpiani A., *Phys. Rev. Lett.*, **95** (2005) 224501.
[24] Canuto C., Hussaini M. Y., Quarteroni A. and Zang T. A., *Spectral Methods : Fundamentals in Single Domains* (Springer, Berlin) 2006.